Available online at www.sciencedirect.com
ScienceDirect
Catalysis Today 137 (2008) 423–428
CATALYSIS TODAY
www.elsevier.com/locate/cattod

Experimental and DFT studies of N_2O decomposition over bare and Co-doped magnesium oxide—insights into the role of active sites topology in dry and wet conditions

Paweł Stelmachowski [a], Filip Zasada [a], Witold Piskorz [a], Andrzej Kotarba [a], Jean-Francois Paul [b], Zbigniew Sojka [a,c,*]

[a] *Faculty of Chemistry, Jagiellonian University, Ingardena 3, 30-060 Kraków, Poland*
[b] *Université des Sciences et Technologies de Lille, Unité de Catalyse et Chimie du Solide UMR 8181, 59655 Villeneuve d'Ascq Cedex, France*
[c] *Regional Laboratory for Physico-Chemical Analyses and Structural Research, Jagiellonian University, Ingardena 3, 30-060 Kraków, Poland*

Available online 21 February 2008

Abstract

Isothermal and TPSR studies of deN_2O reaction were performed over model MgO, and Co–MgO systems. Complementary experiments such as O_2-TPD, H_2O-TPD and IR, supported by DFT molecular modeling were carried out to elucidate the role of topological irregularities such as corners, steps, edges on the principal reaction events in dry and wet environment. The hydroxyl groups produced upon water adsorption were used for selective blocking of the active sites. Topological aspect of the surface reactivity was discussed in terms of the energetics of reaction steps and the relative stability and mobility of reaction intermediates (O_2^{2-}) and inhibiting (OH^-_{surf}) species. Whereas the most active corner sites are depleted by oxygen, produced in the course of N_2O decomposition, the edge and step sites could be eliminated only by more strongly adsorbed water. In steady state conditions the reaction turns over mainly on terrace sites and is moisture insensitive. Upon introduction of Co^{2+} ions to magnesium oxide the N_2O conversion curve is shifted by 200 °C towards lower temperatures, due to the change in the N_2O activation step (from anionic redox to cationic redox). However, at such thermal conditions the terrace sites remain still hydroxylated, and the overall reaction rate is clearly deteriorated by water present in the feed.

Keywords: N_2O; DFT; MgO; Magnesium oxide; Cobalt; Active sites; Morphology; Surface; Hydroxyls; Mechanism

1. Introduction

Nitrous oxide has been identified as a significant contributor to destruction of ozone layer in stratosphere and is also recognized as a relatively strong greenhouse gas [1–4]. Since N_2O is a byproduct in nitric and adipic acids manufactures its decomposition into N_2 and O_2 is a topic of vital interest for environmental chemistry [1,2,5]. Despite of its thermodynamic instability, N_2O is kinetically inert toward direct decomposition into the constituting elements. Thus, this reaction, to be efficient, requires a catalyst for practical applications, especially in the presence of water and oxygen excess usually present in tail gases [2,3]. However, none of the many catalysts developed until now exhibit satisfactory performance in real deN_2O process at the so-called low temperature regime below 350 °C [2,6].

The progress can be made by better understanding of the reaction mechanism including the effect of co-reactants on the active site performance. The principal mechanisms along which the nitrous oxide can be decomposed involve electron transfer [7] and oxygen-atom transfer [8,9]. They are discussed below in more detail. Owing to their simplicity and well known surface chemistry MgO and Co-doped MgO in bare and hydroxylated states are suitable model systems [10–13] for examination of anionic and cationic redox mechanism, respectively [14].

The aim of the study was to elucidate the role of surface topology of MgO matrix in conjunction with effect of water on the course of the deN_2O principal reaction steps. The experimental studies of N_2O decomposition and surface dehydroxylation were corroborated by the DFT molecular modeling.

* Corresponding author. Tel.: +48 12 663 22 95; fax: +48 12 634 05 15.
E-mail address: sojka@chemia.uj.edu.pl (Z. Sojka).

0920-5861/$ – see front matter © 2007 Elsevier B.V. All rights reserved.
doi:10.1016/j.cattod.2007.11.028

2. Experimental

The commercial magnesium oxide provided by Ubichem, with the BET surface area of $S_A = 72.4\ m^2\ g^{-1}$ was used. Magnesium peroxide was obtained by reaction of MgO with 30% H_2O_2 overnight. Cobalt doped magnesium oxide ($Co_{0.05}Mg_{0.95}O$) sample was obtained by impregnation with $Co(NO_3)_2$ obtained from Aldrich followed by the calcination at 700 °C in the flow of He for 12 h.

The samples were characterized by XRD, N_2-BET, IR, O_2-TPD, H_2O-TPD and their deN_2O reactivity was evaluated in isothermal and temperature programmed desorption and surface reaction (TPSR) modes. The phase verification of the materials was performed by the X-ray diffraction using X'pert Pro Philips powder diffractometer with Cu Kα radiation in the Bragg–Brentano geometry. The BET measurements were carried out by means of Quntasorb Junior Instrument. The IR spectra were recorded using a BRUKER IFS 48 spectrometer equipped with an MCT detector with the spectral resolution of $2\ cm^{-1}$. The temperature programmed desorption (TPD) and surface reaction measurements were performed in quartz flow reactor using 500 mg of MgO in the form of sieve fraction of 0.2–0.3 mm. The reactant (5% N_2O in He) flow rate of $7000\ h^{-1}$, and the heating rate of 10 °C/min in the range of 20–900 °C were used. The gas phase composition was monitored by mass spectrometer (SRS RGA200, Stanford Research System). In order to investigate the influence of water on N_2O decomposition the gas feed was additionally saturated with 1 vol.% of H_2O.

For DFT cluster modeling, a 6.3 Å radius hemisphere was cut off from the (1 0 0) plane of MgO, extended next to 20.0 Å by an array of point charges (PC), reproducing the lattice Madelung potential (electrostatic embedding [6]). The stoichiometry of the resultant cluster was $Mg_{40}O_{40}(PC_{1836})$, $Mg_{57}O_{57}(PC_{2060})$, $Mg_{51}O_{51}(PC_{1940})$, $Mg_{53}O_{53}(PC_{2060})$ for modeling sites located at terraces, edges, corners and reverse corners, respectively. The computations were carried out with DMol^3 [15] software with implemented Delley's scheme [16]. The gradient density approximation (GGA) in RPBE parameterization [17] and the DNP basis set with frozen inner core and the integration grid of fine density were used. The geometry optimization was performed for all the ions but those linked directly to at least one PC. The Mayer analysis was used for calculating of bond orders [18]. Transition state geometries were determined following the QLST scheme.

3. Results and discussion

As already mentioned the two basic mechanisms along which N_2O is decomposed over oxide systems involve the anionic redox route initiated by the oxygen-atom transfer and the cationic redox route, triggered by electron transfer [14]. Whereas for bare magnesium oxide the anionic redox mechanism is expected with the principal steps:

$$N_2O + {O^{2-}}_{surf} \rightarrow {O_2^{2-}}_{surf} + N_2$$
(N−O bond breaking via oxygen transfer) (1)

$${O_2^{2-}}_{surf} + {O_2^{2-}}_{surf} \rightarrow 2{O^{2-}}_{surf} + O_2 \quad \text{(oxygen recombination)} \tag{2}$$

for Co–MgO samples the cationic redox mechanism involves:

$$Co^{2+} + N_2O \rightarrow Co^{3+} + O^- + N_2$$
(N−O bond breaking via electron transfer) (3)

$$Co^{3+} + O^- + {O^{2-}}_{surf} \rightarrow Co^{2+} + {O_2^{2-}}_{surf} \quad \text{(oxygen migration)} \tag{4}$$

In both cases the recombination of ${O_2^{2-}}_{surf}$ to produced final O_2 occurs according to Eq. (2). Obviously, some other possible variants of the oxygen migration and recombination steps are also possible invoking the same species.

The reactivity of the MgO catalyst is thus related to the ability of surface oxygen anions to abstract the oxygen atom from N_2O molecule to form O_2^{2-} intermediates. Both steps the atom transfer and recombination of the peroxide ions were modeled by DFT on the principal topological surface irregularities such as terraces, edges, corners and reversed corners. The calculated energy barriers for the oxygen transfer, diffusion from corner and edge sites towards terraces, as well as relative stability of various peroxy ions are listed in Table 1. The latter values were calculated because the diffusion of peroxy intermediates located at edges and corners can occur only through the thermodynamically favourable diffusion of O_2^{2-} toward the terrace sites, where they eventually recombine into dioxygen.

As expected [8,19,20], the results show that the energetics of all these processes is strongly dependent on the surface topology. The barrier for dissociative N_2O activation decreases in the order: terrace (36.2 kcal/mol) > edge (32.2 kcal/mol) > corner (22.4 kcal/mol). Similar trend is observed for

Table 1
Calculated energies for principal surface events and surface species stabilities for various topological locations on MgO in kcal/mol

Energetics of surface events and stability of surface species	Terrace	Edge	Corner/reverse corner
Barrier for oxygen transfer	36.2 (32.4[a], 37.1[b], 38.1[c])	32.2 (31.1[a])	22.4
O_2^{2-} stability	14.2	11.5	3.1
O_2^{2-} recombination	18.9 (25.8[a], 19.6[b])	–	–
Barrier for O_2^{2-} diffusion on/towards terrace	24.6 (25.4[a])	32.3	38.2
OH^- stability	29.7	36.0	42.9/37.3

[a] From reference [20].
[b] From reference [9].
[c] From reference [21].

the relative stability of peroxy intermediates (14 > 11.5 > 3 kcal/mol for terrace, edge and corner, respectively). Whereas for the diffusion of peroxy ions from edges and corners, i.e. the less stable sites towards more stable sites located at terraces, the trend is reversed—terrace (21.1 kcal/mol) < edge (32.3 kcal/mol) < corner (38.3 kcal/mol). The diffusion strictly along the edges involves passage through cations and anions occurring by turns, and such process was found energetically unfavourable. This indicates that the decomposition of nitrous oxide contacted with the bare MgO surface shall start by an incipient attack of N_2O on the lattice oxygen ions located at corners and edges, transforming them via oxygen transfer into peroxy intermediates (Eq. (1)), as the activation energy for oxygen transfer for the most exposed sites is the lowest (Table 1). The resultant corner peroxy ions, however, in spite of the favourable thermodynamic driving force for diffusion towards terraces, will remain rather immobile due to large activation energy for this process. So it may be expected that the sites of the highest coordinative unsaturation are readily eliminated by blocking with the oxygen originating from N_2O dissociation. For the edge sites the activation energies for oxygen transfer and diffusion are very similar (~32 kcal/mol), but smaller than the activation energy for oxygen transfer at terraces (36 kcal/mol). It means that for the edge sites, in contrast to corners, the reaction is expected to be rather independent of the oxygen produced in the N_2O decomposition, as the resultant peroxy intermediates shall exhibit sufficient mobility for recombination.

On terraces the activation of N_2O through oxygen transfer, being energetically the most demanding step, restrains the reaction rate because the recombination of oxygen into O_2 molecules, through diffusion of peroxy intermediates, is energetically relatively easy (Table 1). On the other hand, on corners the situation is reversed. The barrier for oxygen transfer is much lower than for the diffusion of O_2^{2-} that controls the oxygen recombination. As a result, the N_2O decomposition over bare MgO implies that at corners the diffusion of O_2^{2-} is energetically most difficult, on terraces the highest energy barrier was found for N_2O activation, whereas for edges the both processes occur with the similar activation energies. Noting that the latter are significantly smaller by 4–6 kcal/mol than the highest barriers found for corners and terraces, the overall steady state reactivity can be related not only to the less active, but more abundant sites located at terraces, but also to those at edges. This is a different situation than that observed for more basic CaO with larger lattice constant, where in the steady state condition only terraces were supposed to be active [9].

To verify this hypothesis the reaction modeling was corroborated by TPSR studies of N_2O decomposition on MgO, and separately by O_2^{2-} recombination study using MgO_2 as a reference material. Indeed, magnesium peroxide can be treated as a simple model system allowing, through by-passing of the N–O bond breaking step, experimental examination of the surface recombination of peroxy intermediates (Eq. (2)). The results of O_2-TPD of MgO_2 followed by the TPSR of N_2O decomposition are shown in Fig. 1. In the first case two

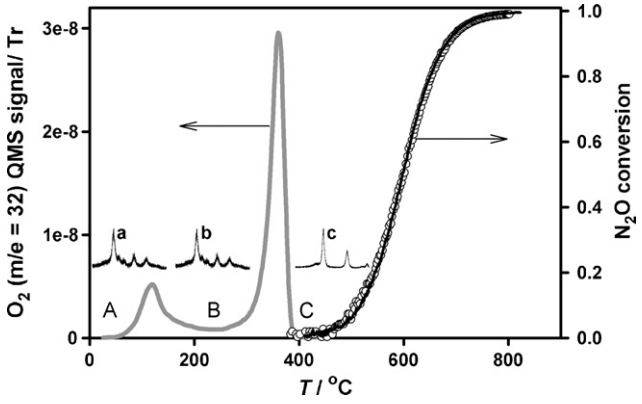

Fig. 1. Results of O_2-TPD from MgO_2 and the TPSR of N_2O decomposition over MgO exMgO_2 and original MgO samples. The changes in the structure of the catalyst material followed by XRD patterns (a–c) are shown in the inserts corresponding to points A–C.

desorption peaks of oxygen can be distinguished. The XRD diffraction patterns, were recorded at temperatures before and after each of the desorption peaks, and are indicated by points A, B, C (vide inserts in Fig. 1a–c). The first desorption maximum, where smaller amounts of oxygen were desorbing, appears at 150 °C and is accomplished at 250 °C (point B). The XRD shows that in this temperature range the bulk MgO_2 structure is still preserved (Fig. 1b). Thus, this peak can be assigned to recombination of surface peroxy anions, described by reaction (2). As a result at point B the surface layer corresponds essentially to nascent MgO, whereas the bulk is still composed of MgO_2 (Fig. 1b). Strong peak of dioxygen generation with the T_{max} at 400 °C indicates that the bulk magnesium peroxide is being vividly transform into MgO at such conditions (vide XRD in Fig. 1c). The sequence of these processes is well reflected in the activation energies of 16 ± 1 kcal/mol for the first maximum (surface O_2^{2-} recombination) and 41 ± 6 kcal/mol for the second one (bulk diffusion), determined by leading edge analysis using various heating rates.

After the complete transformation of peroxy anions into O^{2-} and O_2 the bulk magnesium oxide is eventually formed (Fig. 1c). At 400 °C (point C) the N_2O decomposition over MgO starts and reaches the 100% of conversion at about 700 °C. It is, however, worth noting that the TPSR profile compares quite well with that obtained for original MgO sample (Fig. 1 pointed curve), indicating clearly that the N_2O decomposition is not constrained by the transformation of MgO_2 into MgO. These results show also that the temperature windows for the O_2^{2-} intermediates recombination and N_2O decomposition over MgO are well separated. The oxygen recombination, despite of being a spin forbidden process [14], is apparently easier and takes place at much lower temperatures than the highly activated N–O bond breaking step, which by requiring higher energy, occurs at higher temperature. These findings correlate well with the calculated DFT barriers for N_2O activation (36.2 kcal/mol) and O_2^{2-} recombination (18.9 kcal/mol) processes (Table 1). It is worth noting that the latter value compares quite well with the experimental one (16 kcal/mol),

showing that the O_2 desorption from MgO_2 provides a quite reliable approach for exploring the reaction step (2) on MgO surface.

Following the molecular modeling data the N_2O activation and O_2^{2-} recombination steps strongly depend on the topology of the active sites. A straightforward implication from the DFT data is that at the isothermal conditions, in the course of N_2O decomposition the small initial decrease in the conversion by ~2%, shown in Fig. 2a, can be accounted for by gradual depletion of the active sites of the highest coordinative unsaturation [9], because in such a case the O_2^{2-} diffusion is blocked.

According to [13,21] participation of the sites located at corners, edges and terraces can be controlled by their selective blocking through hydroxylation, by making use of distinctly different thermal stability of the corresponding OH groups (Fig. 3). The calculated stabilization energies for surface hydroxyls produced upon dissociative adsorption of water at different locations vary from 29.7 to 42.9 kcal/mol (Table 1). These results, together with the corroborative IR measurements and previous literature [22,23,13], may be used to interpret the TPD profile of water desorption from MgO, where several peaks can be distinguished (Fig. 4). The low temperature peak in the range of 100–150 °C corresponds to the surface dehydration of the sample, in accordance with the concomitant diminishing of the broad IR band (3100–3600 cm^{-1}) due to hydrogen bonded OH species. The TPD peak in the range 200–300 °C can be assigned to dehydroxylation of terraces, observed also as the decrease in the IR intensities of the hydrogen bonded and free hydroxyls at 3650–3720 cm^{-1}. The weak broad maximum above 600 °C we assigned to dehydroxylation of edges and corners in accordance with the highest stability of the corresponding OH groups, revealed by the DFT results and the literature [22,23,13]. The effective blocking of these exposed sites by hydroxyls can be revealed from the N_2O decomposition over hydoxylated MgO surface, shown in Fig. 2b. At 600 °C practically only the edge and corner hydroxyls can persist and their accumulation in time was followed by QMS (Fig. 2c). The depletion of active sites at corners and edges leads to the conversion decay of ~20%. This effect is much more pronounced than in the case of oxygen, which being the reaction product could also block the less abundant surface corner sites (Fig. 2a). Indeed, for all topological sites the stability of the hydroxyl groups are much higher than that of the peroxy species, therefore once the OH group is formed the corresponding active site is effectively eliminated, not only from the N_2O activation but also from O_2^{2-} diffusive recombination. As a result the N_2O decomposition over MgO is rather insensitive to water in the TPSR experiment (Fig. 5a and a′). Indeed, before the temperature of the appreciable conversion is reached (see Fig. 1), the elapsed time (40 min for heating rate of 10 °C/min) is sufficient for complete saturation of the edge and corner active sites with

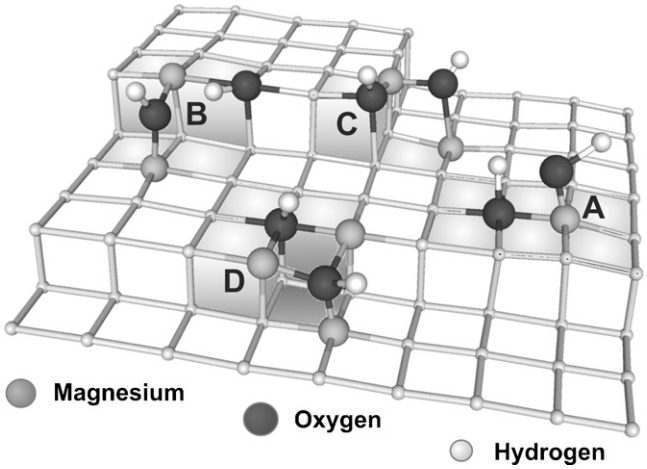

Fig. 3. Model of MgO surface showing various positions and DFT structures of OH^- groups on topological irregularities: A—terrace, B—edge, C—corner, D—reverse corner.

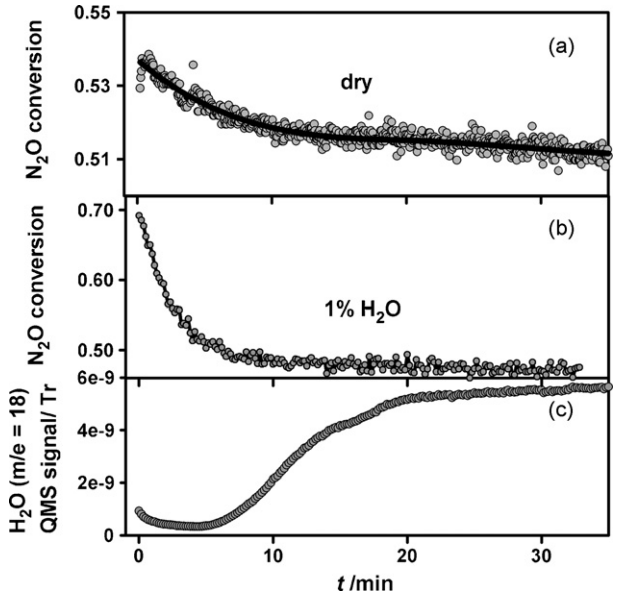

Fig. 2. Isothermal conversion of N_2O as a function of time in dry (a) and 1% of H_2O (b) atmosphere over MgO at 550 and 600 °C, respectively along with the associated simultaneous H_2O adsorption followed by QMS (c). For wet feed the reaction temperature was enhanced to maintain the similar level of N_2O conversion.

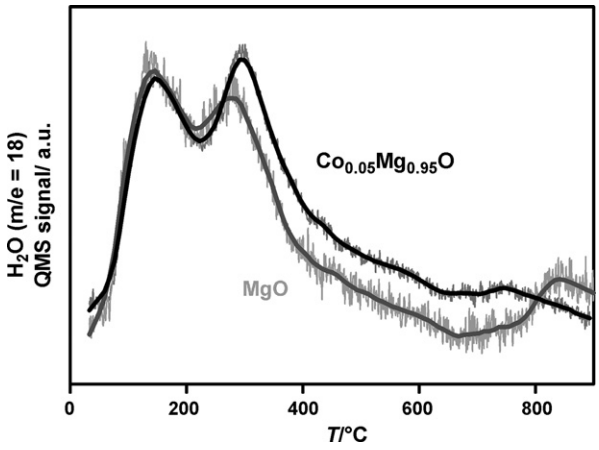

Fig. 4. QMS-TPD of water from MgO and Co-doped MgO surfaces.

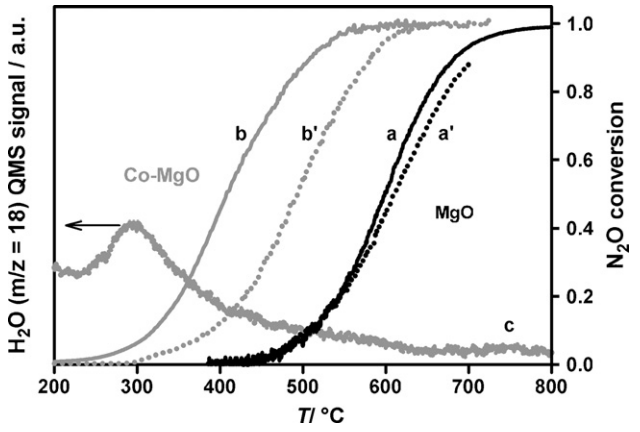

Fig. 5. The effect of water on the N_2O conversion over MgO (a—dry, a′—1% H_2O atmosphere) and Co-doped MgO (b—dry, b′—1% H_2O atmosphere) catalysts together with the superimposed fragment of H_2O-TPD profile (c) for Co–MgO sample.

hydroxyls when water is present in the feed. This can be inferred from the isothermal experiments (Fig. 2). In TPSR measurements, the most stable OH groups located at edges/steps, corners and reversed corners (Fig. 3b–d) persist on the MgO surface in the whole temperature range of the N_2O decomposition (Fig. 5). They are experimentally observed in the H_2O-TPD as a desorption maximum above 800 °C (Fig. 4). As a result the TPSR profile is not sensitive to water present in the feed, since in the reaction temperature window the terrace hydroxyls are already unstable (thus, the terrace active sites can participate in this reaction), whereas the most active sites located on morphological irregularities remain blocked by OH groups during the whole measurement (Fig. 5). On the contrary, in the isothermal experiments over bare (hydroxyl free) MgO, the initial activity is steadily declining by simultaneous gradual accumulation of water on the surface, until a steady state is reached, which at 600 °C takes about 10–15 min (Fig. 2).

By doping the MgO sample with Co the mechanism of N_2O activation can be changed from that based on oxygen transfer (Eq. (1)) into that based on electron transfer (Eq. (3)), where the electron is provided by the Co^{2+} donor centers. Since the 5 mol% of Co corresponds to the lowest value of the work function for the whole range of the Co–MgO solid solution (i.e. to the highest electron donor ability of the resultant material) [24], this level of doping was used in the experiments. Definitely, introduction of Co into MgO matrix drastically improved the catalytic deN_2O activity, as shown in Fig. 5a and b, where for 50% conversion the shift of 200 °C towards lower temperature is observed. In contrast to pristine MgO (Fig. 5a and a′), the Co–MgO catalyst is much more sensitive to the presence of 1% water in the feed (Fig. 5b and b′). Comparison of the deN_2O-TPSR results with the superimposed H_2O-TPD curve for Co–MgO (Fig. 5c) indicates that once the surface is progressively clean up from hydroxyls, the N_2O decomposition gradually develops. The temperature range for water desorption indicates that in this case the removal of water takes place mainly from terraces. Thus, the number of terrace Co^{2+} redox sites available for the reaction is effectively controlled by the actual OH surface coverage. As a result the beneficial enhancement of reactivity of the terraces by switching the anionic redox activation of N_2O into the cationic one, is considerably revoked by co-adsorbed water. It could be, however, at least partly retained by better controlling of the surface hydrophobicity, the work in this direction is in progress.

4. Conclusions

Two mechanistic models, an anionic redox and a cationic redox, were used to discuss the surface reactivity of MgO and Co–MgO in N_2O decomposition process. The pronounced topological aspect of the surface reactivity and sensitivity towards water was investigated by complementary O_2-TPD, H_2O-TPD and IR experiments and rationalized by the DFT molecular modeling.

It has been shown that the most active corner sites of MgO are readily depleted by transformation into stabile O_2^{2-} species, whereas the edge sites can be effectively blocked only by dissociatively co-adsorbed water. The steady state reactivity of MgO in dry conditions involves the predominant, but the least active, terrace sites as well as the less abundant, but more active edge sites. The N_2O decomposition over MgO occurs at the temperature range, where the terraces are virtually dehydroxylated, and only the partaking edge sites, which can be effectively obstructed by water, make the N_2O decomposition slightly moisture sensitive at such thermal conditions. Although upon doping of MgO by Co^{2+}, the temperature of the reaction can readily be decreased by 200 °C (owing to engagement of the cationic redox mechanism), in that case the terrace sites are to a great extent hydroxylated when water is present in the feed, and the reaction rate is strongly inhibited.

Acknowledgement

This work has been supported by the project PBZ-MEiN-3/2/2006.

References

[1] M. Iwamoto, H. Hamada, Catal. Today 10 (1991) 57.
[2] F. Kaptein, J. Rodriguez-Mirasol, J.A. Moulijn, Appl. Catal. B 9 (1996) 25.
[3] C.S. Swamy, J. Christofer, Catal. Rev. -Sci. Eng. 34 (1992) 409.
[4] B. Moden, P. Da Costa, B. Fonfe, D. Ki Lee, E. Iglesia, J. Catal. 209 (2002) 75.
[5] E.V. Kondratenko, J. Pérez-Ramirez, Catal. Today 121 (2007) 197.
[6] J.H. Lunsford, The Catalytic Chemistry of Nitrogen Oxides, Plenum, New York, 1975.
[7] Z. Sojka, M. Che, J. Phys. Chem. 100 (1996) 14776.
[8] E.J. Karlsen, M.A. Nygren, L.G.M. Pettersson, J. Phys. Chem. A 106 (2002) 7868.
[9] A. Satsuma, R. Akahori, M. Kato, S. Komai, H. Yoshida, T. Hattori, J. Mol. Catal. A 155 (2000) 81.
[10] E. Giamello, Z. Sojka, M. Che, A. Zecchina, J. Phys. Chem. 90 (1986) 6084.
[11] P. Martino, M.M. Chiesa, C. Paganini, E. Giamello, Surf. Sci. 527 (2003) 80.

[12] M. Sterrer, T. Berger, O. Diwald, E. Knözinger, P.V. Sushko, A.L. Shluger, J. Chem. Phys. 123 (2005) 1.
[13] C. Chizallet, G. Costentin, M. Che, F. Delbecq, P. Sautet, J. Am. Chem. Soc. 129 (2007) 6442.
[14] P. Pietrzyk, F. Zasada, W. Piskorz, A. Kotarba, Z. Sojka, Catal. Today 119 (2007) 219.
[15] DMol3, Quantum-chemical software, Molecular Simulations, Inc., 1999.
[16] B. Delley, J. Chem. Phys. 92 (1990) 508.
[17] B. Hammer, L.B. Hansen, J.K. Norskov, Phys. Rev. B 59 (1999) 7413.
[18] I. Mayer, Chem. Phys. Lett. 97 (1983) 270.
[19] A. Scagnelli, S. Di Valentin, G. Pacchioni, Surf. Sci. 600 (2006) 386.
[20] A. Snis, H. Miettinen, J. Phys. Chem. B 102 (1998) 2555.
[21] O. Diwald, M. Sterrer, E. Knözinger, Phys. Chem. Chem. Phys. 4 (2002) 2811.
[22] S. Coluccia, E. Garrone, E. Borello, J. Chem. Soc. Faraday Trans. 1 (79) (1983) 607.
[23] E. Knözinger, K.H. Jacob, S. Singh, P. Hofmann, Surf. Sci. 290 (1993) 388.
[24] K. Dyrek, Z. Sojka, Stud. Surf. Sci. Catal. 21 (1985) 195.